AFRL-RB-WP-TR-2008-3090

MULTI-OBJECTIVE EVOLUTIONARY STRUCTURAL OPTIMIZATION USING COMBINED STATIC/DYNAMIC CONTROL PARAMETERS

Delivery Order 0007

Ramana V. Grandhi, Woo-Young Kim, and Mark A. Haney

Wright State University

APRIL 2007
Interim Report

AIR FORCE RESEARCH LABORATORY
AIR VEHICLES DIRECTORATE
WRIGHT-PATTERSON AIR FORCE BASE, OH 45433-7542
AIR FORCE MATERIEL COMMAND
UNITED STATES AIR FORCE

NOTICE AND SIGNATURE PAGE

Using Government drawings, specifications, or other data included in this document for any purpose other than Government procurement does not in any way obligate the U.S. Government. The fact that the Government formulated or supplied the drawings, specifications, or other data does not license the holder or any other person or corporation; or convey any rights or permission to manufacture, use, or sell any patented invention that may relate to them.

This report was cleared for public release by the Air Force Research Laboratory Wright-Patterson Air Force Base (AFRL/WPAFB) Public Affairs Office and is available to the general public, including foreign nationals. Copies may be obtained from the Defense Technical Information Center (DTIC) (http://www.dtic.mil).

AFRL-RB-WP-TR-2008-3090 HAS BEEN REVIEWED AND IS APPROVED FOR PUBLICATION IN ACCORDANCE WITH ASSIGNED DISTRIBUTION STATEMENT.

*//Signature//

MARK A. HANEY
Aerospace Engineer
Structural Mechanics Branch

*//Signature//

ANDREW G. SPARKS, Chief
Structural Mechanics Branch
Structures Division

*//Signature//

DAVID M. PRATT, Ph.D.
Technical Advisor
Structures Division

This report is published in the interest of scientific and technical information exchange, and its publication does not constitute the Government's approval or disapproval of its ideas or findings.

*Disseminated copies will show "//signature//" stamped or typed above the signature blocks.

REPORT DOCUMENTATION PAGE

Form Approved
OMB No. 0704-0188

1. REPORT DATE *(DD-MM-YY)*	2. REPORT TYPE	3. DATES COVERED *(From - To)*
April 2007	Interim	12 September 2006 – 20 March 2007

4. TITLE AND SUBTITLE
MULTI-OBJECTIVE EVOLUTIONARY STRUCTURAL OPTIMIZATION USING COMBINED STATIC/DYNAMIC CONTROL PARAMETERS
Delivery Order 0007

5a. CONTRACT NUMBER
FA8650-04-D-3446-0007

5b. GRANT NUMBER

5c. PROGRAM ELEMENT NUMBER
0602201

6. AUTHOR(S)
Ramana V. Grandhi and Woo-Young Kim (Wright State University)
Mark A. Haney (AFRL/RBSM)

5d. PROJECT NUMBER
A0B7

5e. TASK NUMBER

5f. WORK UNIT NUMBER
0A

7. PERFORMING ORGANIZATION NAME(S) AND ADDRESS(ES)

Wright State University
Department of Mechanical and Materials Engineering
3640 Colonel Glenn Highway
Dayton, OH 45435-0001

Structural Mechanics Branch (AFRL/RBSM)
Structures Division, Air Force Research Laboratory
Air Vehicles Directorate
Wright-Patterson Air Force Base, OH 45433-7542
Air Force Materiel Command, United States Air Force

8. PERFORMING ORGANIZATION REPORT NUMBER

9. SPONSORING/MONITORING AGENCY NAME(S) AND ADDRESS(ES)

Air Force Research Laboratory
Air Vehicles Directorate
Wright-Patterson Air Force Base, OH 45433-7542
Air Force Materiel Command
United States Air Force

10. SPONSORING/MONITORING AGENCY ACRONYM(S)
AFRL/RBSM

11. SPONSORING/MONITORING AGENCY REPORT NUMBER(S)
AFRL-RB-WP-TR-2008-3090

12. DISTRIBUTION/AVAILABILITY STATEMENT
Approved for public release; distribution unlimited.

13. SUPPLEMENTARY NOTES
PAO Case Number: WPAFB 08-1717, 27 Mar 2008. Report contains color.

14. ABSTRACT
A thermal protection system (TPS) is responsible for protecting a spacecraft's components from melting due to high reentry temperatures. In the design of TPS, both maximum thermal stress and minimum natural frequency must be considered due to the combined thermoacoustic environment inherent in high-speed vehicle applications. A multiobjective structural optimization method for the three-dimensional acreage TPS design is developed using an evolutionary structural optimization (ESO) algorithm. The static control parameter used to find the optimum in minimum thermal stress design is modified to address an irregular mode-switching phenomenon, as well as to improve the modal stiffness in dynamic analysis. Two objectives are optimized simultaneously, namely, the maximization of fundamental natural frequency and the minimization of maximum thermal stress. The proposed modified control parameter is demonstrated in the design of a metallic TPS using the method of weighted objectives. The results are then compared with the conventional ESO sensitivity approach. This work concludes by applying the methodology which makes use of both topology and shape optimization in the design of an acreage TPS.

15. SUBJECT TERMS
Thermal Protection System, Evolutionary Structural Optimization, topology optimization

16. SECURITY CLASSIFICATION OF:			17. LIMITATION OF ABSTRACT:	18. NUMBER OF PAGES	19a. NAME OF RESPONSIBLE PERSON (Monitor)
a. REPORT	b. ABSTRACT	c. THIS PAGE			Mark A. Haney, Ph.D.
Unclassified	Unclassified	Unclassified	SAR	38	19b. TELEPHONE NUMBER *(Include Area Code)* N/A

Standard Form 298 (Rev. 8-98)
Prescribed by ANSI Std. Z39-18

Table of Contents

PAGE

LIST OF FIGURES…….iv

ACKNOWLEDGEMENT……..…..v

1. SUMMARY ……. 1

2. INTRODUCTION …….….. 2

3. SENSITIVITY ANALYSIS ……..……4

3.1 Control Parameter for Static Analysis ……..……...4

3.2 Control Parameter for Dynamic Analysis……..……...4

4. MULTI-OBJECTIVE OPTIMIZATION TECHNIQUE ...……..…….8

5. EVOLUTIONARY STRUCTURAL OPTIMIZATION ALGORITHM …….. 9

6. THERMAL PROTECTION SYSTEMS DESIGN……10

6.1 Example 1: TPS Model with External Forces……..10

6.2 Example 2: TPS Model with Heat Transfer Considerations…… 11

6.2.1 Availability of the Proposed Control Parameter in the Heat Transfer Problem..…….12

6.2.2 TPS Design with Heat Transfer Problem…….14

7. CONCLUSIONS…….. 16

8. REFERENCES……. 17

NOMENCLATURE……..…27

LIST OF FIGURES

PAGE

Figure 1. An initial metallic TPS…….. 18
Figure 2. Relationship between the fundamental natural frequency and the maximum stress. 19
Figure 3. Evolutionary histories of the fundamental natural frequencies and the maximum thermal stress……20
Figure 4. Resultant TPS models with 900 Hz fundamental natural frequency…….21
Figure 5. Initial model for designing TPS support……22
Figure 6. Evolutionary histories for TPS support design……. 23
Figure 7. Optimum TPS support……...24
Figure 8. Evolutionary history of the fundamental natural frequency for TPS frame design.. 25
Figure 9. Optimum TPS model including heat transfer effects…… 26

ACKNOWLEDGEMENT

The first two authors would like to acknowledge the U.S. Air Force for supporting this research through the contract FA8650-04-D-3446-0007.

1. SUMMARY

A Thermal Protection System (TPS) is responsible for protecting a spacecraft's components from melting due to high re-entry temperatures. In the design of TPS, both maximum thermal stress and minimum natural frequency must be considered due to the combined thermo-acoustic environment inherent in high-speed vehicle applications. In this work, a multi-objective structural optimization method for the three-dimensional acreage TPS design is developed using an Evolutionary Structural Optimization (ESO) algorithm. The static control parameter used to find the optimum in minimum thermal stress design is modified to address an irregular mode-switching phenomenon, as well as for improving the modal stiffness in dynamic analysis. Two objectives are optimized simultaneously; namely, the maximization of fundamental natural frequency and the minimization of maximum thermal stress. The proposed modified control parameter is demonstrated on the design of a metallic TPS using the method of weighted objectives. The results are then compared with the conventional ESO sensitivity approach. This work concludes by applying the methodology which makes use of both topology and shape optimization in the design of an acreage TPS.

2. INTRODUCTION

The primary challenges that must be addressed to enable lower-cost access to space are weight, reusability, and ease of maintenance. The current methodology for the design of space and high speed air vehicles is to construct a low-temperature load bearing structure and then to apply a thermal protective layer [also known as a Thermal Protection System (TPS)] whose purpose is to shield the low temperature structure. A successful TPS will not only perform its primary function of maintaining the underlying vehicle structure within acceptable temperature limits, but must also be durable, operable, cost effective, and lightweight. By its very nature, TPS is parasitic. Current research efforts in "hot" structures are investigating the feasibility of using advanced structural materials that can provide both structural rigidity and survivability in the high-temperature environment. No conclusion has yet been reached which of the two approaches will prove to be the most efficient. Hence, continued research into parasitic TPS is extremely relevant.

Existing TPS consists of different types of materials that are distributed over the spacecraft. These various thermal insulators consist of felt blankets, ceramic blankets, ceramic tiles, carbon-carbon leading edges, as well as metallic TPS. Metallic TPS has obvious advantages and disadvantages; the nature and response of metals is well understood. Furthermore, the durability and fracture toughness of metals are generally much greater than that of ceramics. One disadvantage of metallic systems is weight. This work attempts to mitigate this effect through weight minimization.

The metallic TPS design for a spacecraft operating in extreme environments of thermal and acoustic loading is of significant importance.[1] Design considerations for thermal and acoustic loading conditions tend to be at odds with one another. Floating or compliant designs will tend to reduce thermal stresses, whereas less compliant designs increase natural frequency and avoid excitation from wide-band random engine noise. To address the TPS design efficiently, optimization methods are essential both from the standpoint of identifying a potentially small feasible region and driving toward low weight designs.

Traditional structural topology optimization methods, such as the density-based method,[2] the Homogenization method,[3, 4] and the Evolutionary Structural Optimization (ESO) method,[5, 6] are applicable to multi-objective optimization problems concerned with static or dynamic problems. Multi-objective optimization is the method of forming a solution that satisfies a number of conflicting objectives in the "best" way possible. That is, multi-objective optimization is the generation of a design that achieves the optimum performance of the structure while consideration is given to various criteria.[7, 8] The solution to the multi-objective problem is known as a Pareto optimum.[8, 9] Pareto optima are not unique solutions, but rather they consist of a series of solutions.[10]

This paper incorporates the multi-objective optimization problem into the ESO algorithm using the weighted objectives technique. The ESO method developed by Xie and Steven in 1992 slowly removes inefficient material from a structure, and the residual shape of the structure evolves as an optimum.[5] The ESO procedure does not address the mode-switching phenomenon that is common in three-dimensional dynamic problems. Mode-switching is a phenomenon that changes the ordering of natural modes with structural modification. The phenomenon often occurs between the natural mode of interest and the neighboring orthogonal natural modes. The natural frequency of interest and the modal stiffness are drastically affected, resulting in convergence difficulties and/or non-optimal configurations. In two-dimensional

structures, Xie and his colleagues attempted to prevent the phenomenon by increasing the separation between frequencies.[11] However, this method is not applicable to three-dimensional structures in which the phenomenon occurs unpredictably during design iterations. In addition, as the number of elements eliminated increases during the iterative ESO process, a sudden drop in the natural frequency of interest is observed. This is a direct result of the modal stiffness decrease associated with the current level of element removal. The ESO method and the associated dynamic sensitivity number[5] fail to consider modal stiffness directly. Consequently, these problems make it harder for the ESO method to determine the Pareto optimum in the multi-objective optimization[6] that contains dynamic characteristics.

In this paper, the modified static control parameter using von Mises stress is newly formulated to prevent non-smooth changes in modal stiffness and the associated natural frequency of interest. This modified static control parameter smooths the iterative process by introducing correlation between the natural mode of interest and its neighboring modes, as well as a consideration of the modal stiffness. Using the proposed control parameter, the ESO method results in a lightweight TPS model with improved static and dynamic characteristics even though the mode-switching phenomena are observed frequently in the iterative steps. These improvements are accomplished through efficient material volume reduction.

In the next section, control parameters for static and dynamic analysis based on von Mises stress are formulated. Section III presents the details of the multi-objective optimization technique. The evolutionary optimization algorithm is described in Section IV. In section V, two relevant metallic TPS models with different load cases are presented to demonstrate the applicability of the ESO method with the proposed control parameter.

3. SENSITIVITY ANALYSIS

Like most other structural optimization methods, the ESO method must be iterated many times. It is important to search for the removal positions where the effect is high for achieving the objective as accurately and quickly as possible. In this section, two kinds of control parameters (called sensitivity numbers[5]), based on static analysis are presented as guidelines for the removal of the finite elements. In particular, the modified static control parameter is newly developed to reduce the problems of the weakness of the modal stiffness and the mode-switching phenomenon in dynamics.

3.1 Control parameter for Static Analysis

The stress level in each element can be measured by an average of all of the stress components. For this purpose, the von Mises stress has been one of the most frequently used criteria for isotropic materials. The von Mises stress σ_l^{vm} of the l^{th} element for a three-dimensional structure is defined as

$$\sigma_l^{vm} = \frac{1}{\sqrt{2}}\sqrt{\left(\sigma_{x,l}-\sigma_{y,l}\right)^2+\left(\sigma_{y,l}-\sigma_{z,l}\right)^2+\left(\sigma_{z,l}-\sigma_{x,l}\right)^2+6\left(\tau_{xy,l}^2+\tau_{yz,l}^2+\tau_{zx,l}^2\right)} \qquad (1)$$

Here, $\sigma_{x,l}$, $\sigma_{y,l}$, and $\sigma_{z,l}$ are normal stresses of the l^{th} element in x, y, and z directions, respectively, and $\tau_{xy,l}$, $\tau_{yz,l}$, and $\tau_{zx,l}$ are the shear stresses of the l^{th} element.

According to the ESO algorithm, a reliable sign of potential structural failure is excessive stress or strain, and a low stressed element is assumed to be under-utilized in the structure. Ideally, the stress in every part of a structure should be near the same safe level. By gradually removing material that has a lower stress, the stress level in the new designs become more and more uniform. By defining the von Mises stress as the static control parameter in the static analysis, a number of elements with the smallest static control parameter are removed so that the increase of the maximum von Mises stress is minimal. The removal process must be slightly modified when the stresses are primarily thermally induced.[12]

3.2 Control parameter for Dynamic Analysis

The dynamic control parameter in the ESO method [5, 11] is derived from the Rayleigh quotient and is based on the natural mode of interest. This control parameter estimates only the change of the natural frequency of interest. No direct consideration is given to the modal stiffness. Also, when mode-switching is observed during the optimization process, the characteristic of the dynamic control parameter varies drastically due to the change in the natural mode of interest. These effects can make the modal stiffness very small bringing about a drastic change in the natural frequency of interest when a large number of elements are eliminated from the structure through many iterative steps.

To address the shortcomings of the traditional ESO method, a static control parameter using von Mises stress is developed, which gives direct consideration to the modal stiffness as a substitute for the conventional dynamic control parameter based on the Rayleigh quotient. In addition, this *static* control parameter is modified so that consideration is given to adjacent natural modes, as well as the natural mode of interest thus preventing a rapid change in the characteristic of the control parameter.

The derivation of the modified *static* control parameter for dynamics is as follows. The equation of motion for an undamped system is described by

$$[M]\{\ddot{x}\}+[K]\{x\}=\{f\} \tag{2}$$

where $[M]$ and $[K]$ are the global mass matrix and global stiffness matrix, respectively, and $\{x\}$ and $\{f\}$ are the global nodal displacement and nodal force vectors, respectively. The displacement in the spatial coordinates of Eq. (2) can also be expressed using the modal coordinates by

$$\{x\}=\varepsilon_1\{\Phi_1\}+\varepsilon_2\{\Phi_2\}+\cdots+\varepsilon_N\{\Phi_N\}=[\Phi]\{\varepsilon\} \tag{3}$$

where *N* is the total number of degrees of freedom, and $\{\Phi\}$ and $\{\varepsilon\}$ represent natural modes and modal displacements, respectively.

Using Eq. (3) and the characteristics of generalized orthogonality, the response in the spatial coordinates is derived as

$$\{x\}=\sum_{r=1}^{N}\frac{\{\Phi_r\}\{\Phi_r\}^T\{F\}}{-\omega^2 m_r+k_r}\,e^{j\omega t} \tag{4}$$

where ω is the natural frequency, $\{\Phi_r\}^T[M]\{\Phi_r\}=m_r=1$, $\{\Phi_r\}^T[K]\{\Phi_r\}=k_r$, and $\{f\}=\{F\}e^{j\omega t}$.

In this method, the displacement of each nodal point is computed by implementing the concept of a virtual static displacement for each mode shape. The virtual static displacement is chosen to be the same displacement shape as that of the mode shape. The displacement for each mode shape is derived by assuming $\omega = 0$. The absolute value of the displacement is given by

$$\begin{aligned}\{x\}&=\sum_{r=1}^{N}\frac{\{\Phi_r\}\{\Phi_r\}^T\{F\}}{k_r}\\&=[\Phi][k_r]^{-1}[\Phi]^T\{F\}\end{aligned} \tag{5}$$

Note that $[k_r]=diag(k_1,\cdots,k_N)$. From Eq. (5), $[k_r]^{-1}[\Phi]^T\{F\}$ indicates a modal displacement that is generated by the external force $\{F\}$. The natural mode $\{\Phi_r\}$ can be treated as a response (displacement) by applying the external force whose modal displacement is 1 for the r^{th} mode and 0 for other modes. When $\{F_r\}$ is the external force satisfying this condition, $\{F_r\}$ is easily obtained by the relationship between the displacement and external force, as shown in Eq. (6):

$$\{F_r\} = [K]\{\Phi_r\} \tag{6}$$

In general, the magnitude of the external force will vary from mode to mode, with higher natural modes requiring larger external forces due to the complexity of the higher mode shapes. This tendency is exploited in the development of a novel control parameter which simultaneously considers all frequencies of interest. The hypothesis uses relative force magnitudes as a surrogate for "closeness" of natural frequencies. The nodal force vectors are scaled such that large nodal forces (corresponding to complicated mode shapes) are reduced by the factor $\left(\|F_i\|/\|F_r\|\right)^P$. Thus $\{F_r\}_{new}$ is given by Eq. (7):

$$\{F_r\}_{new} = \left(\frac{\|F_i\|}{\|F_r\|}\right)^P \{F_r\} \tag{7}$$

Here, subscript i shows the order of interest, ($0 < i << N$). Exponent P, which adjusts the magnitude of the scaling factor between the i^{th} natural mode and the r^{th} natural mode, is the correlation factor (typically P = 1). A larger value of P emphasizes the relative importance of the natural mode of interest. The same scaling can be used for the response

$$\{\Phi_r\}_{new} = \left(\frac{\|F_i\|}{\|F_r\|}\right)^P \{\Phi_r\} \tag{8}$$

The scaled eigenvectors $\{\Phi_r\}_{new}$ are then applied as static displacement fields.

Using Eqs. (1) and (8), von Mises stresses of each element are obtained from the i^{th} natural mode to the n^{th} natural mode. Each natural mode is used as a displacement vector, and the stress components for each natural mode are obtained by using the strain-displacement and stress-strain relations. Finally, for each finite element, the maximum von Mises stress value between the i^{th} and the n^{th} natural modes is selected as the new dynamic control parameter, as expressed by Eq. (9).

$$\sigma_l^{vm} = \max\left\langle \sigma_{i,l}^{vm}, \sigma_{i+1,l}^{vm}, \sigma_{i+2,l}^{vm}, \cdots, \sigma_{n,l}^{vm} \right\rangle \qquad (0 < i << n,\ n < N) \tag{9}$$

Since Eq. (9) considers not only the i^{th} natural frequency, but also its neighboring natural frequencies, the smooth change of natural frequency can be possible even if mode-switching occurs in the iterative processes. For example, when other natural frequencies are much higher than the i^{th} natural frequency, only the maximum von Mises stress of the i^{th} natural mode is selected for each finite element because $\left(\|F_i\|/\|F_r\|\right)^P$ for other natural modes has small values (<<1). On the other hand, as the neighboring natural frequencies approach that of the i^{th} natural frequency during the iterative process, other natural modes are also gradually considered (i.e., $\left(\|F_i\|/\|F_r\|\right)^P \cong 1$). Note that it is not necessary to consider lower frequencies than the i^{th} natural frequency because they don't switch with the i^{th} natural frequency in most cases.

Since the proposed dynamic control parameter is derived by using the von Mises stress, a number of elements having some of the smallest von Mises stresses, that is, the most inefficient elements are removed from the structure, identical to the static optimization problem of the ESO method.

4. MULTI-OBJECTIVE OPTIMIZATION TECHNIQUE

In the weighted objectives method, this multi-objective problem is converted to a single-objective problem by using a weighted sum of the original multiple objectives. That is, the control parameter for the static characteristic in Eq. (1) and the control parameter for the dynamic characteristic in Eq. (9) are combined together to form a new single criterion:

$$F_l^{multi} = W_1 R_{1,\,l} + W_2 R_{2,\,l} = \sum_{j=1}^{2} W_j R_{j,\,l} \tag{10}$$

where F_l^{multi} is the multi-objective function that determines element removal for each element *l*. W_j is the j^{th} criterion weighting factor with $0 \le W_j \le 1$ and $\sum_{j=1}^{2} W_j = 1$. $R_{j,l} = \sigma_{j,\,l}^{vm} \big/ \sigma_{j,\,\max}^{vm}$ is the ratio of the j^{th} criterion control parameter $\sigma_{j,\,l}^{vm}$ for the l^{th} element to the maximum value of the j^{th} criterion control parameter $\sigma_{j,\,\max}^{vm}$. Since both control parameters are derived from von Mises stress, a number of elements with the smallest F_l^{multi} are removed so that both characteristics can be improved, as in the conventional ESO method for statics.

5. EVOLUTIONARY STRUCTURAL OPTIMIZATION ALGORITHM

The ESO algorithm of the weighted objectives method for stress and the fundamental natural frequency is implemented as follows:

i) Discretize the structure using a fine mesh of finite elements.
ii) Solve the linear static analysis problem under thermal loads (or mechanical loads).
iii) Calculate the von Mises stress by using Eq. (1).
iv) Solve the eigenvalue problem.
v) Calculate the von Mises stress by using Eq. (9).
vi) Combine the two control parameters by using Eq. (10).
vii) Remove several elements from the current structure that have relatively small contributions.
viii) Repeat steps ii) to vii) until the weight of the structure reaches the predetermined value.

The typical ESO process is operated by a rejection ratio (RR) that determines which elements to eliminate. During the iterative process, the rejection ratio is gradually increased by the evolutionary rate (ER).[5] The rejection ratio is simply implemented by comparing the relative reference levels of candidate elements with the maximum value. In general, the maximum value of the reference criterion doesn't decrease during the evolutionary process for most mechanical load cases. This allows the threshold levels to steadily increase with material removal. Conversely, for cases involving thermal stress, the maximum stress level can decrease as the evolutionary process progresses.[12] For this reason, a new rejection ratio RR_{new} is determined as the α^{th} lowest F^{multi} value. Note that α should be sufficiently small to guarantee a smooth change between two iterations. In this method, α is set to 1~2% of the total number of elements for the initial iteration.

6. THERMAL PROTECTION SYSTEMS DESIGN

Because the TPS comprises the external surface of a spacecraft, several requirements must be satisfied to design a TPS for all environments experienced by the vehicle:

a) In order to minimize operational costs, a TPS should be as lightweight as possible while maintaining its stiffness and high natural frequency.
b) A thin TPS plate is needed to protect a spacecraft from heat, and a frame structure may be attached to prevent fluttering due to aerodynamic and/or acoustic loading. If required, a honeycomb sandwich can be affixed to the plate if the spacecraft encounters a maximum surface temperature for an extended period of time.
c) A long support connecting the plate to the fuselage is recommended to decrease heat transfer to the fuselage. This construction provides for extra volume of insulation to be placed in the cavity, and facilitates the generation of novel attachment by ESO (or other topology) methods.
d) The maximum thermal stress in the TPS is required to remain below yield strength to avoid permanent deformation.

In this section, two relevant TPS models with different initial conditions are presented to demonstrate the effectiveness of the ESO method with the proposed control parameter. An efficient means for designing a TPS is shown for various requirements by employing the proposed control parameter. The initial TPS design is shown in Fig. 1. Inconel alloy 693 is utilized because of its excellent resistance to metal dusting and high temperature corrosion, as well as for its favorable fabrication and joining properties.[13] The TPS models are discretized with hexahedron isoparametric linear elements for finite element analysis, and the p-version of the linear finite element method with Guyan reduction is applied to enhance the accuracy of the analysis and reduce computational effort.[14] Structural characteristic matrices with more degrees of freedom are generated, although the sizes of the matrices are identical to those obtained with the h-version finite element method. For both examples, α, a parameter for the element removal, as shown in the previous section, is set at 1%, and n in Eq. (9) is set at 10.

6.1 Example 1: TPS Model with External Forces

The conventional ESO method and the new ESO method with the proposed control parameter are both applied to a TPS model with a mechanical load case. The TPS model, which has the dimensions of A=0.5 m, B=0.45 m, C=0.03 m, and D=0.27 m, as shown in Fig. 1, is loaded at room temperature, with a Young's modulus of 196 GPa, a material density of 7770 kg/m^3, and a Poisson's ratio of 0.32. The model is meshed with 0.05 m$\times$0.05 m$\times$0.03 m rectangular isoparametric elements with fixity prescribed on the bottom side. External tractions of magnitude 10 N in the X direction are applied to each nodal point on the top side. The elements identified with the external force, which include those in the plate-frame region, are set as unremovable elements. This unremovable region renders the evolutionary process unstable in the conventional ESO method as adjacent regions with high modal mass are eliminated without consideration of the modal stiffness.

The optimization problem is to minimize the maximum von Mises stress and to maximize the fundamental natural frequency while reducing the TPS weight. These two objectives are applied as weighted objectives as shown in Eq. (10). The relationship between maximum von

Mises stress and the fundamental natural frequency is investigated by varying both weighting factors and volume reduction.

Figure 2 shows the comparison between the fundamental natural frequency and the maximum von Mises stress when reductions in volume are 20% and 50%. The plots show results for both the conventional ESO[6] and the proposed method. The weighting factor for the dynamic characteristic ($W_{dynamic}$) and the weighting factor for the static characteristic (W_{static}) for each point in Fig. 2 are as follows:

(A) and (A'): $W_{dynamic} : W_{static} = 0.0:1.0$,

(B) and (B'): $W_{dynamic} : W_{static} = 0.2:0.8$,

(C) and (C'): $W_{dynamic} : W_{static} = 0.5:0.5$,

(D) and (D'): $W_{dynamic} : W_{static} = 0.8:0.2$,

(E) and (E'): $W_{dynamic} : W_{static} = 1.0:0.0$.

Points of (A)-(E) and (A')-(E') are results from the conventional and the proposed method, respectively.

In the proposed method, it is observed that each objective is improved by increasing its respective weighting factor (e.g. both the fundamental natural frequency and the maximum von Mises stress increase when the dynamic weighting factor is increased and the static weighting factor is decreased). Because the proposed method applied to the modified static control parameter directly considers the mode-switching phenomenon and the modal stiffness, smooth changes are observed in the static and dynamic characteristics even as a large number of elements are removed through many iterations. It is shown that any improvement of one criterion requires a clear tradeoff with the other, and a clear Pareto solution (or a Pareto curve) can be observed.

Unlike the proposed method, a desirable solution is not obtained in the conventional method. As shown in Fig. 2, the maximum von Mises stresses obtained with the conventional method are higher than those obtained from the proposed method with increasing $W_{dynamic}$. Even though the conventional method addresses the relative ratio between modal stiffness and modal mass, the deficiency arises from no *direct* consideration of modal stiffness. In addition, it is shown that the fundamental natural frequencies at $W_{dynamic} : W_{static} = 1.0:0.0$ are decreased by this lack of modal stiffness as well as the changing control parameter characteristics due to mode-switching. Determining the trend of the Pareto solution with volume reduction is extremely difficult. Consequently, compared with the conventional method, the proposed control parameter for an eigenvalue problem can be used to design an optimum structure that requires the elimination of a large number of elements through many iterative processes in addition to favorable dynamic modification.

6.2 Example 2: TPS Model with Heat Transfer Considerations

When a spacecraft re-enters the atmosphere from Low Earth Orbit, a metallic TPS creates a temperature distribution due to tremendous heat flux. The temperature distribution changes the material characteristics of a metallic TPS, such as thermal conductivity, Young's modulus, etc. This temperature dependence in the thermal problem results in nonlinearity and requires an iterative solution technique.

For the second example, a transient conduction analysis is applied to the initial TPS model in Fig. 1. It is assumed that the [void] space inside the TPS and the vertical surface boundaries (with the exception of the surface of the plate) are insulated. The plate temperature (T_{plate}) on the top side varies according to a temperature profile, as shown in Ref. 15. In this method, the temperature is simply represented as $T_{plate} = 1.2540t + 200$ (°C) when $t < 500$ (sec.), and $T_{plate} = 827$ (°C) when $t \geq 500$ (sec.), regardless of the elimination of elements from the structure. This assumption is a severe restriction. In the true structure, convection and radiation play major roles in the transfer of energy. For instance, to address the internal radiative heat transfer that will occur as material is removed, an efficient method for constructing view factors during the iterative process would be needed. Since the purpose of this work was to develop an ESO method for simultaneous consideration of thermal stress and frequency, prescribed temperature boundary conditions were used to ensure tractability.

A numerical time integration scheme,[16] similar to Newmark's method, is used to solve the following transient heat transfer problem

$$\left(\frac{1}{\Delta t}[M_t] + \beta[K_t]\right)\{T_{i+1}\} = \left[\frac{1}{\Delta t}[M_t] - (1-\beta)[K_t]\right]\{T_i\} + (1-\beta)\{F_i\} + \beta\{F_{i+1}\} \qquad (11)$$

where $[M_t]$: Consistent-mass matrix

$[K_t]$: Thermal conductivity matrix

$\{F_i\}$: Force matrix defined by heat source (or heat sink), heat flux, and convection

Δt: Time step

β: Parameter, which is set as 0.5 by the Crank-Nicolson rule

$\{T_i\}$, $\{T_{i+1}\}$: Temperatures at time t_i and t_{i+1}, respectively

To reduce the computational time of the transient analysis, only the tendency of the temperature profile at t=1500 (sec.) is evaluated by assuming that $[M_t]$ and $[K_t]$ as constant with time as thermal conductivities ($K_{xx} = K_{yy} = K_{zz}$ = 20 W/(m-°C)), density (ρ=7770 kg/m^3), and specific heat (c=530 J/(kg-°C)) are treated as temperature-independent variables. A constant time of Δt=10 sec. is considered. The initial temperature distribution $\{T_0\}$ for each iterative process is assumed to be a linear profile through the thickness with 127 °C on the top side and 27 °C on the bottom side.

6.2.1 Availability of the Proposed Control Parameter in the Heat Transfer Problem

Both conventional and proposed methods are compared to demonstrate the applicability of the proposed control parameter for topology optimization of a TPS. The TPS model has the dimension of A=0.48 m, B=0.42 m, C=0.03m, and D is specifically set as 0.27 m longer than conventional structures[17] to reduce thermal stress in the fixed regions at the bottom side (interface to low-temperature material). The plate and frame regions are treated as unremovable. The model is divided into 0.03 m×0.03 m×0.03 m regular hexahedron isoparametric elements, and the 0.06 m×0.06 m bottom corner regions are considered fixed. The coefficient of expansion and Young's modulus are considered as functions of temperature.[13] In much the same way as

Example 1, the weighted objectives method considers both the maximum thermal stress and the fundamental natural frequency by changing both weighting factors and volume reduction.

Figure 3 shows the changes in fundamental natural frequencies and maximum thermal stresses by varying weighting factors and sensitivities. Both methods improve the fundamental natural frequencies by increasing the weighting factors for dynamics, as in the mechanical load case. In general, when a structure is over-designed, in other words, when a structure consists of more elements than needed, the fundamental natural frequency can be increased by removing inefficient elements. However, when the stiffness of the structure becomes weak, the fundamental natural frequency is decreased. In Fig. 3, as a large number of elements are removed from the structure through many iterative steps, the proposed method keeps the fundamental natural frequencies much higher than that obtained from the conventional method, even though there is no inertia consideration in the proposed control parameter. Conversely, the results using the conventional control parameter show that the fundamental natural frequency decreases quickly due to (1) the small modal stiffness in the connecting region between the assumed fixity and the plate-frame region and (2) the characteristic change in the control parameter due to the discontinuous change in the natural modes (i.e., mode-switching phenomenon).

On the other hand, the analysis of the change in the maximum thermal stress reveals different behavior when compared with the mechanical load case. A higher static weighting factor does indeed result in a lower maximum thermal stress. In the conventional method, the minimization of the maximum thermal stress can be obtained by applying a large weighting factor for the static control parameter in the early stages of the analysis, similar to the mechanical load case. As the volume removal percentage increases, the maximum thermal stress that results from dynamic considerations alone becomes less than the maximum thermal stress that results from static considerations alone. These seemingly inconsistent results are due to heat transfer considerations. With constant temperature boundary conditions prescribed, the heat flux to the bottom side is decreased with the elimination of elements that connect the plate-frame to the support region. The results from the proposed method have analogous tendencies to the conventional method with changing weighting factors. However, the proposed method can restrain the maximum stresses for $W_{dynamic} : W_{static} = 1.0 : 0.0$ from increasing at early stages of the process.

Figure 4 shows resulting models close to 900 Hz in fundamental natural frequency by both the conventional and proposed methods. Each model is developed using solely dynamic considerations, that is, $W_{dynamic} : W_{static} = 1.0 : 0.0$. The fundamental natural frequency, maximum stress, and the number of elements result in 933.6 Hz, 0.523 GPa, and 740 (155.2 kg) using the conventional method, and 906.8 Hz, 0.330 GPa, and 568 (119.2 kg) by the proposed method. The main difference between the two resulting topologies is the location of the elements that are adjacent to the plate-frame region: one is located towards the center of the plate-frame region, and the other is located towards the edges of the plate-frame region.

From the above results, the ESO method with the proposed control parameter can be used to design a lightweight TPS model with a high fundamental natural frequency and a low maximum thermal stress. Using the assumption that only conduction affects the support region, a practical TPS design is developed by using $W_{dynamic} : W_{static} = 1.0 : 0.0$ in the next section.

6.2.2 TPS Design with Heat Transfer Problem

In contrast to the static case, the convergence of the eigenvalue maximization problem presents a more daunting task. In an evolutionary optimization that requires a large number of element removals through many iterative steps, the ordering of natural modes can be altered by the selection of the initial geometry. This input can result in considerable variations to the problem's structural characteristics (i.e. neighboring natural frequencies, weight of the structure, etc.). Therefore, based on the topology results of the previous section (Fig. 4 (b)), the initial TPS model is chosen to be that of Fig. 4 (b) with a slight modification. Element are removed from inside the structure, as shown in Fig. 5. The shape optimization method using the ESO technique (called 'nibbling ESO'[5]) is then applied to the support region to avoid the checkerboard pattern that occurred in Fig. 4 (b). That is, only the structural boundaries in the Z direction between Layer 1 and Layer 10 (with the exception of the unremovable region of Layer 0) are removed from the model. The frame region, as well as the support region, is designed to reduce the TPS weight. Using the proposed method, the objectives take the following form:

Minimize TPS weight

subject to

1. maximization of the fundamental natural frequency ($f_1 \geq 900$ Hz)
2. minimization of the maximum thermal stress below yield strength ($\sigma_{\max} \leq 0.3$ GPa)

In early iterations, the fundamental natural mode is the bending mode of the support region. The elements of the frame part are eliminated to improve the dynamic characteristics of the support. The local bending mode of the thin top plate becomes the lowest mode of the structure. If the original model was too coarse or too much material was removed at each iteration, the plate may not satisfy the frequency constraint and could result in undesirable flutter or acoustic excitation. The problem becomes a multi-scale phenomenon. Inefficient material still exists in the base but the optimization algorithm is focusing on the low frequency of the plate. Therefore, to address the problem efficiently, the design optimizations for the support region and the frame region are conducted separately.

TPS Support Design

First, the support region for the initial model in Fig. 5 is set up with identical boundary conditions and mesh size, as with that of previous section V.B.1. However, additional fixed regions are established at the edges of the plate to prevent a local mode from occurring in the unremovable region due to dynamic considerations. By including additional stiffness [k_X, k_Y, k_Z] = [0, 0, 10^8] (N/m), the local mode of the unremovable region will have a higher natural frequency when compared with the fundamental natural frequency of the support's first bending mode. Figure 6 shows the change in the fundamental natural frequency and the maximum thermal stress as a function of volume reduction, which is the ratio percentage between the current and the fully-populated structure's volume. For this case, the structure at 77.7% volume removal is the most lightweight that satisfies the two constraints (Fig. 7). When additional stiffness is removed from the plate, the fundamental natural frequency is less than 900 Hz due to the increase in modal mass of the unremovable region. In this case, the TPS model has the fundamental natural frequency of 871.9 Hz, and the maximum thermal stress occurs in the support region.

TPS Frame Design

Using the modified TPS model in Fig. 7, the model is then designed to be lightweight with the fundamental natural frequency greater than 900 Hz by modifying the frame shape. In the frame design, it is possible to increase the fundamental natural frequency because all elements in the frame region have a high fundamental modal mass. The modal stiffness of the plate and the frame can be also considered by applying the proposed control parameter. The plate and the frame regions are remeshed with two element sizes, $0.03\ \text{m} \times 0.03\ \text{m} \times 0.007\ \text{m}$ in the frame and $0.03\ \text{m} \times 0.03\ \text{m} \times 0.002\ \text{m}$ in the plate. As in the element size of the plate, the thickness is set at 0.002 m. The four corners at the bottom of the support region are assumed fixed as in the example of Section V.B.1. Shape optimization is applied by eliminating elements from the bottom surface of the frame region for ease of manufacture, as with the support design. Because the maximum thermal stress exists in the support region, no thermal stress analysis is applied. Only the temperature profile of the TPS model in Fig. 7 is utilized for the evaluation of the material properties.

Figure 8 shows the evolutionary history of the fundamental natural frequency due to modifications of the frame region. Up to the 41^{st} iteration, the fundamental frequency increases because excessive modal mass is removed from the frame. Then, the frequency drastically decreases because the modal stiffness is reduced by the lack of elements in the frame region, even though the frame has excessive modal mass. In the frame design, the modified TPS model satisfies the frequency constraints at the 45^{th} iteration, and has a fundamental natural frequency of 920.2 Hz.

Finally, a transient heat transfer analysis is applied to the TPS model at the 45^{th} iteration for the evaluation of the exact solution. In this case, the model has the fundamental natural frequency of 919.8 Hz, the maximum thermal stress of 0.228 GPa, and 816 elements (76.50 kg), which consist of 224 elements (3.13 kg) in the plate, 316 elements (15.47 kg) in the frame, and 276 elements (57.90 kg) in the support region. The fundamental natural frequency is reduced slightly by the change of the material properties, and the maximum thermal stress is also reduced slightly by the volume reduction of the frame. The final modified TPS model and the cross-section of the frame-plate are shown in Fig. 9. To prevent flutter of the plate, it is shown that the stiffness of the center region on the plate is reinforced by the existence of the elements in the frame, even though the elements have a high modal mass about the natural mode of the plate.

7. CONCLUSIONS

A metallic TPS concept provides the possibility of decoupling the thermal and structural functions by providing metallic substructures to encapsulate internal insulation, maintain panel shape, and support thermal and mechanical loads. This decoupling allows the use of structurally efficient internal insulations. However, these two functions can not be decoupled perfectly, so each substructure in the metallic TPS model should be designed to reduce thermal defects, as well as to allow for structural modification.

In this paper, a multi-objective optimization problem for the thermal stress and the fundamental natural frequency was conducted to make a lightweight TPS model by using the Evolutionary Structural Optimization (ESO) algorithm. Two objectives were optimized simultaneously, namely, the maximization of the fundamental natural frequency and the minimization of the maximum thermal stress, through efficient volume reduction. Specifically, the modified static control parameter based on static analysis was newly proposed for the TPS design concerned with dynamic analysis. Through the comparison between the conventional and the proposed control parameter, it was shown that the proposed control parameter can prevent several problems, which are induced by failing to consider the mode-switching phenomenon and the reduced modal stiffness directly when a large number of elements are eliminated through many iterative steps (although the proposed control parameter ignores inertia terms of the equation of motion). Additionally, an efficient way to obtain a metallic TPS model was shown by designing the frame and the support region separately using the ESO method with the proposed control parameter. In future work, consideration will be given to more realistic thermal conditions. Inclusion of convection and radiation as well as a maximum temperature constraint will potentially result in new and innovative designs.

8. REFERENCES

[1]Penmetsa, R. C., Grandhi, R. V., and Haney, M., "Topology Optimization for Evolutionary Design of Thermal Protection System," *AIAA Journal of Spacecraft and Rockets*, Submitted 2004.

[2]Bendsoe, M. P., "Optimal Shape Design as a Material Distribution Problem," *Structural Optimization* 1989, *1*, 193-202.

[3]Bendsoe, M. P. and Kikuchi, N., "Generating Optimal Topologies in Structural Design Using a Homogenization Method," *Computer Methods in Applied Mechanics and Engineering* 1988, *71*, 197-224.

[4]Ma, Z. -D., Kikuchi, N., and Chang, H. -C., "Topological Design for Vibrating Structures," *Computer Methods in Applied Mechanics & Engineering* 1995, *121*(1-4), 259-280.

[5]Xie, Y. M. and Steven, G. P., Evolutionary Structural Optimization; Springer-Verlag: London, 1997.

[6]Proos, K. A., Steven, G. P., Querin, O. M., and Xie, Y. M., "Multicriterion Evolutionary Structural Optimization Using the Global Criterion Methods," *AIAA Journal* 2001, *39*(10), 2006-2012.

[7]Grandhi, R. V., Bharatram, G., and Venkayya, V. B., "Multiobjective Optimization of Large Scale Structures," *AIAA Journal* 1993, *31*(7), 1329-1337.

[8]Carmichael, D. G., "Computation of Pareto Optima in Structural Design," *International Journal for Numerical Methods in Engineering* 1980, *15*(6), 925-952.

[9]Das, I. and Dennis, J. E., "A Closer Look at Drawbacks of Minimizing Weighted Sums of Objectives for Pareto Set Generation on Multicriteria Optimization Problems," *Structural Optimization* 1997, *14*, 63-69.

[10]Pietrzak, J., "Pareto Optimum Tests," *Computers and Structures* 1999, *71*(1), 35-42.

[11]Xie, Y. M. and Steven, G. P., "Evolutionary Structural Optimization for Dynamic Problems," *Computers & Structures* 1996, *58*(6), 1067-1073.

[12]Li, Q., Steven, G. P., and Querin, O. M., "Structural Topology Design with Multiple Thermal Criteria," *Engineering Computations*, 2000, *17*(6), 715-734.

[13]INCONEL® alloy 693 – Excellent Resistance to Metal Dusting and High Temperature Corrosion, http://www.specialmetals.com/documents/Inconel%20alloy%20693.pdf (accessed Jan 2005).

[14]Kim, W. -Y., Nakahara, T., and Okuma, M., "An Evolutionary Optimization Method for Designing the Three-Dimensional Structures," *Transaction of Japan Society for Computational Engineering and Science* 2003, *5*(1), 25-31.

[15]Blosser, M. L. "Thermal Protection Systems for Reusable Launch Vehicles," *14th Annual Thermal & Fluids Analysis Workshop*, Hampton, VA, August 18-22, 2003.

[16]Logan, D. L., A First Course in the Finite Element Method – 3rd ed.; Brooks/Cole: USA, 2000.

[17]Blosser, M. L., Martin, C. J. Daryabeigi, K., and Poteet, C. C., "Reusable Metallic Thermal Protection Systems Development," *Third European Workshop on Thermal Protection Systems*, Noordwijk, The Netherlands, March 25-27, 1998.

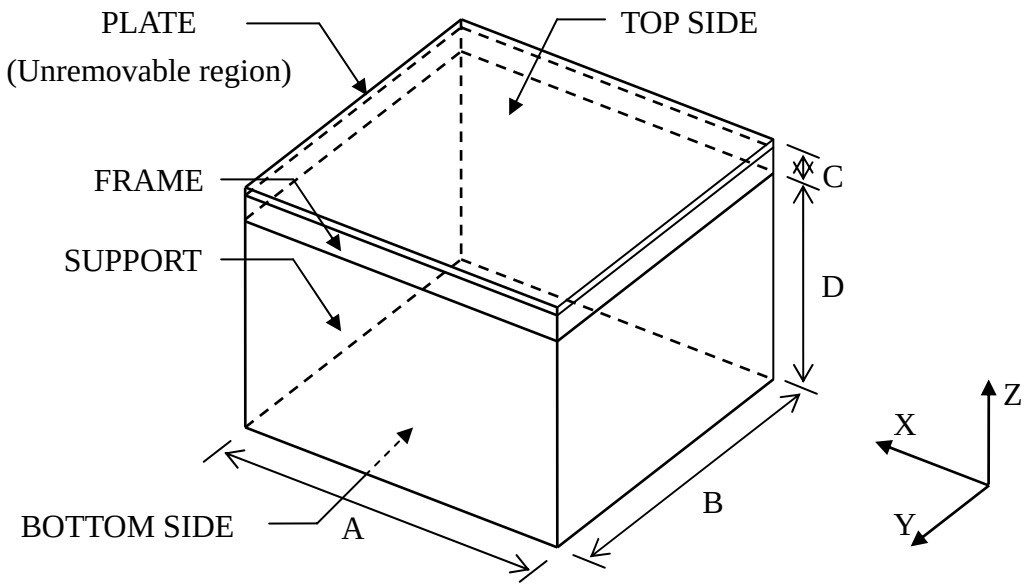

Fig. 1 An initial metallic TPS

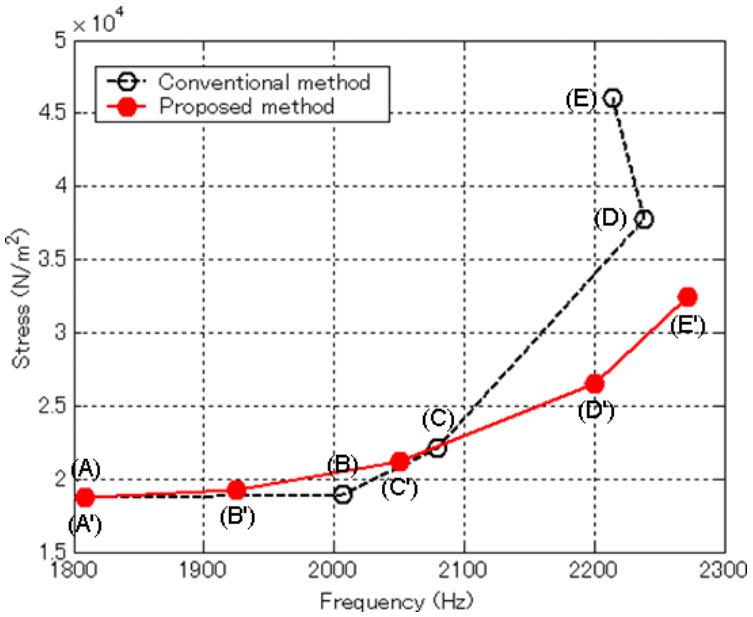

(a) 20% volume reduction

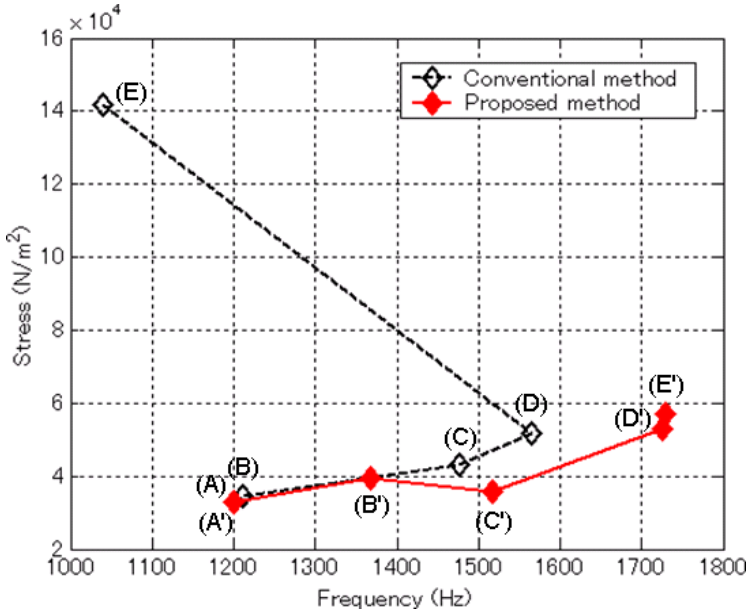

(b) 50% volume reduction

Fig. 2 Relationship between the fundamental natural frequency and the maximum stress

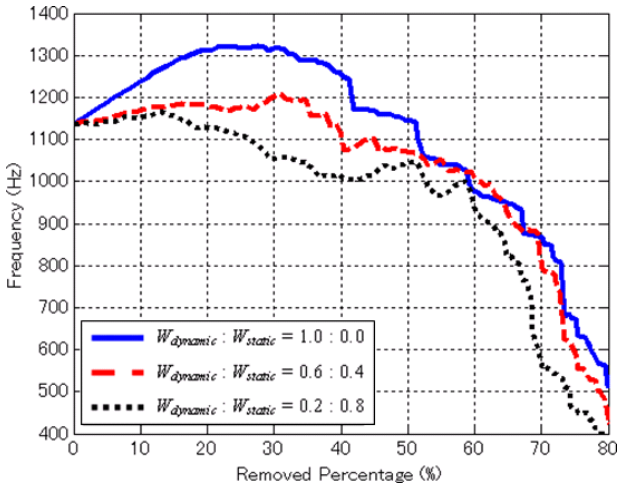

(a) Frequency histories by the conventional method

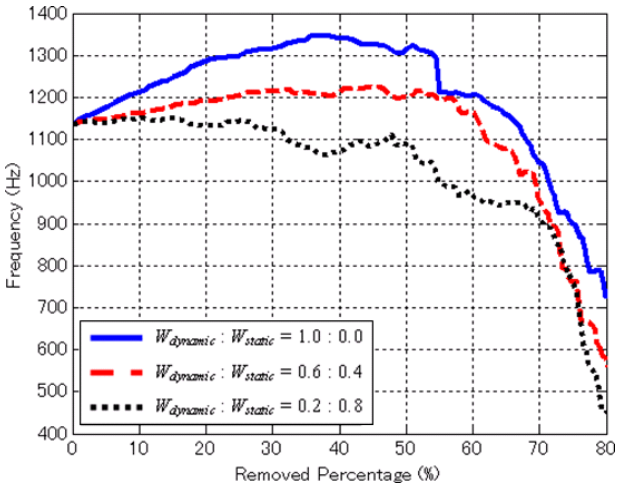

(b) Frequency histories by the proposed method

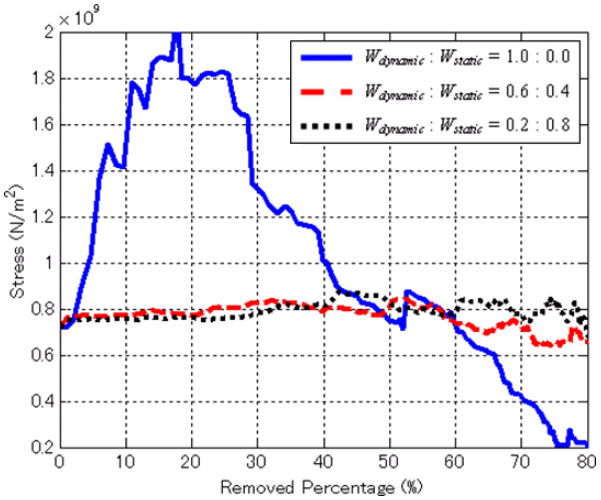

(c) Max. stress histories by the conventional method

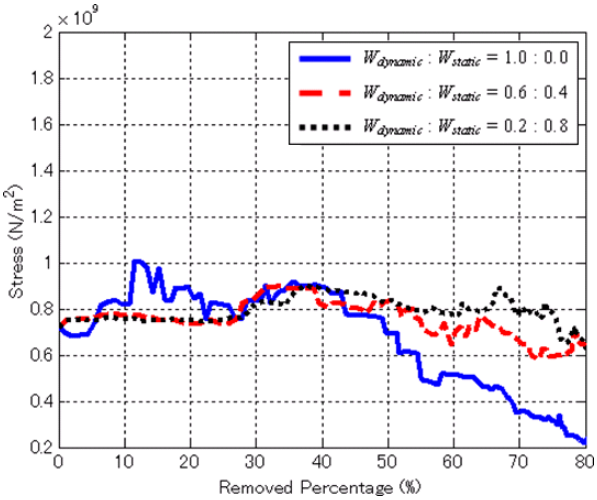

(d) Max. stress histories by the proposed method

Fig. 3 Evolutionary histories of the fundamental natural frequencies and the maximum thermal stress

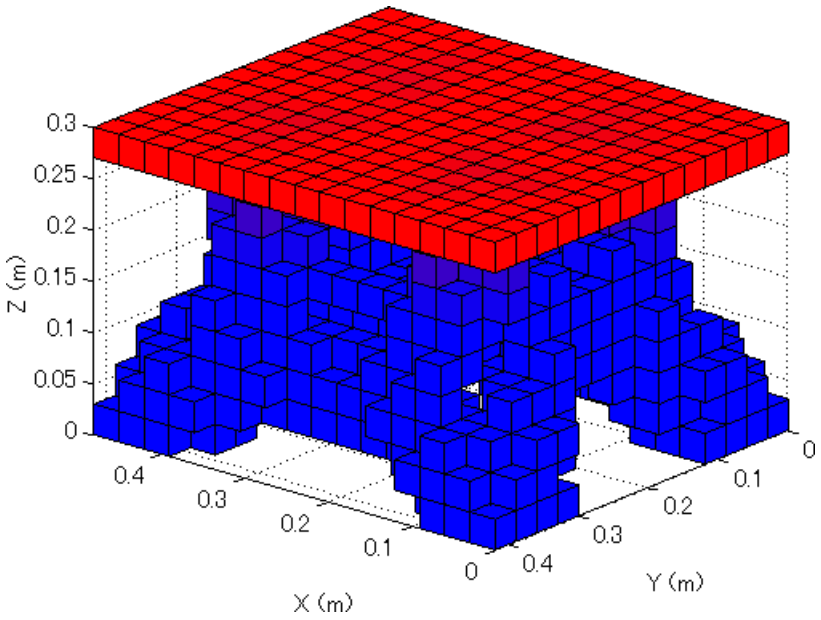

(a) Modified TPS model by the conventional method

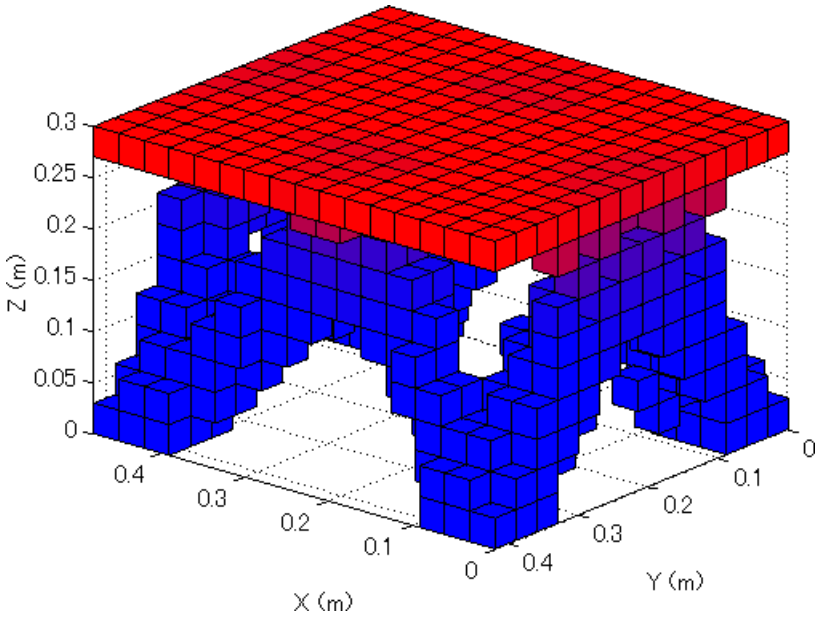

(b) Modified TPS model by the proposed method

Fig. 4 Resultant TPS models with 900 Hz fundamental natural frequency

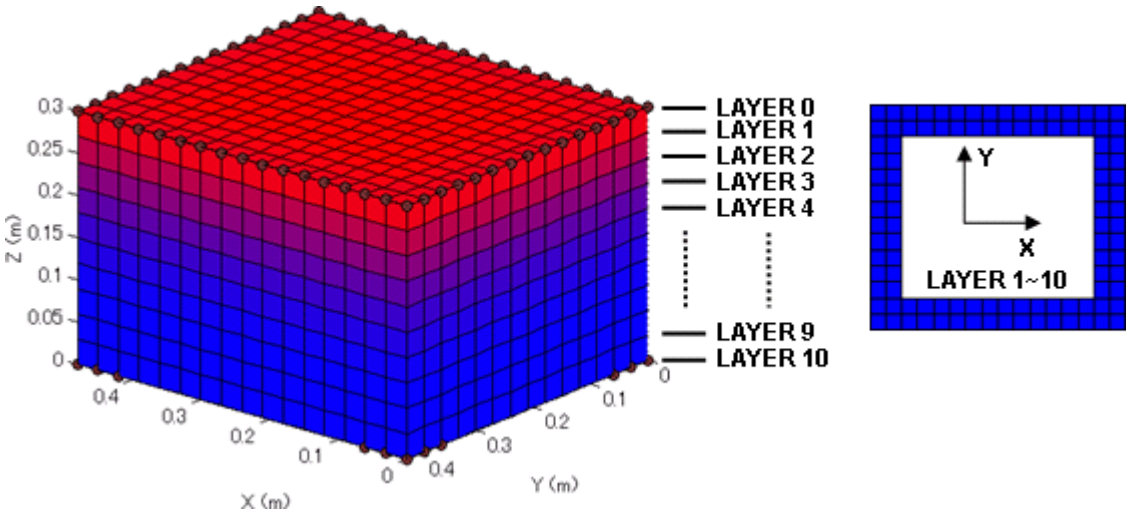

Fig. 5 Initial model for designing TPS support

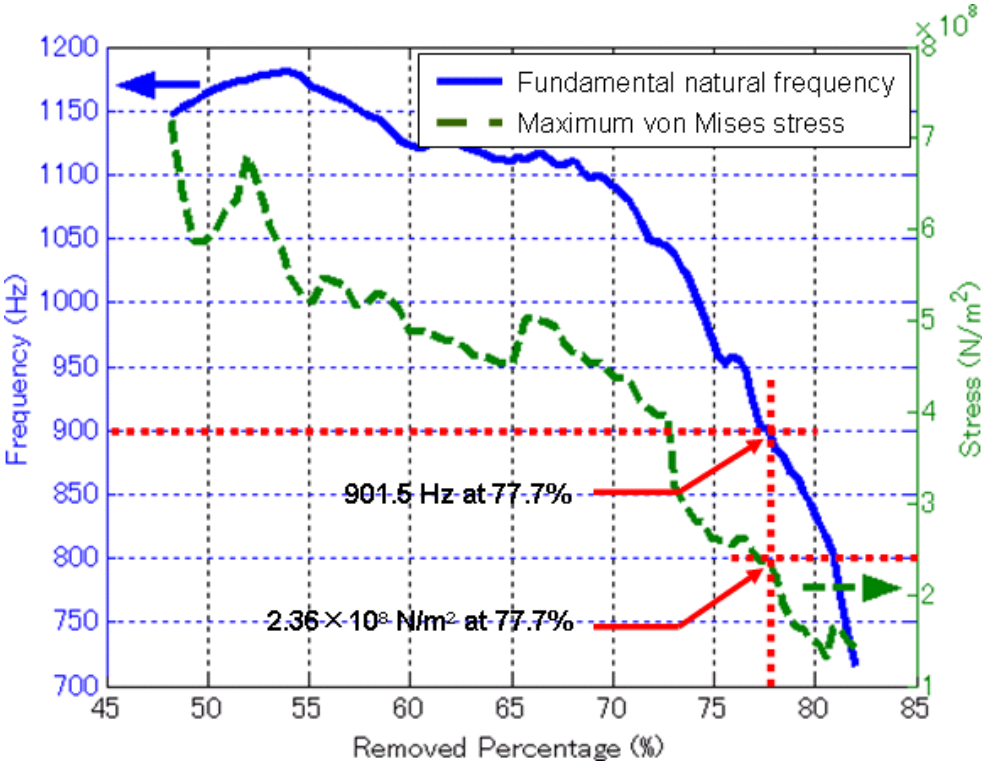

Fig. 6 Evolutionary histories for TPS support design

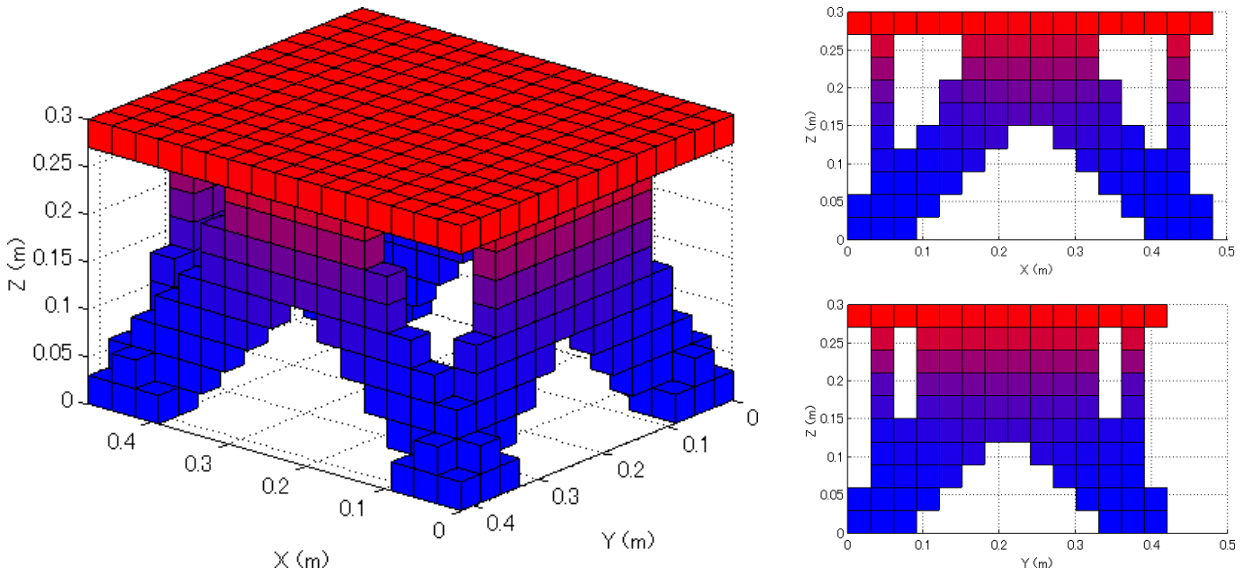

Fig. 7 Optimum TPS support

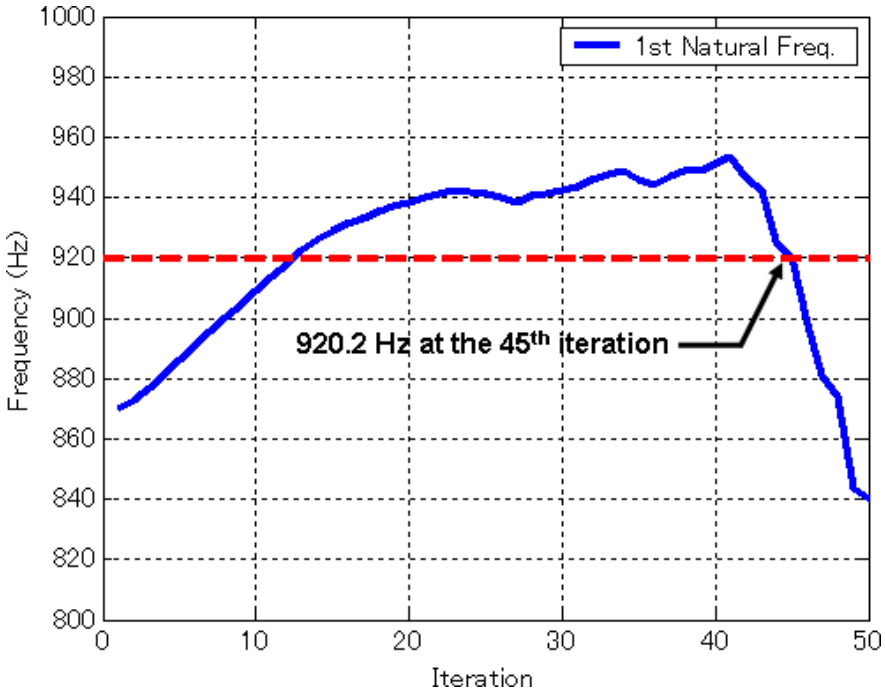

Fig. 8 Evolutionary history of the fundamental natural frequency for TPS frame design

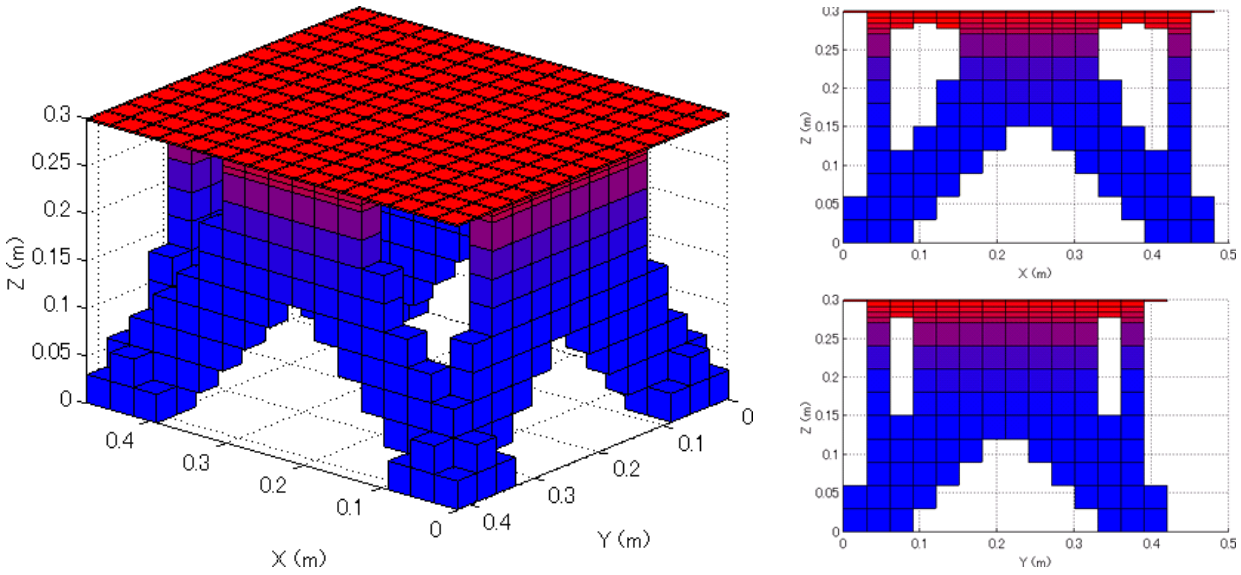

(a) Optimum TPS model

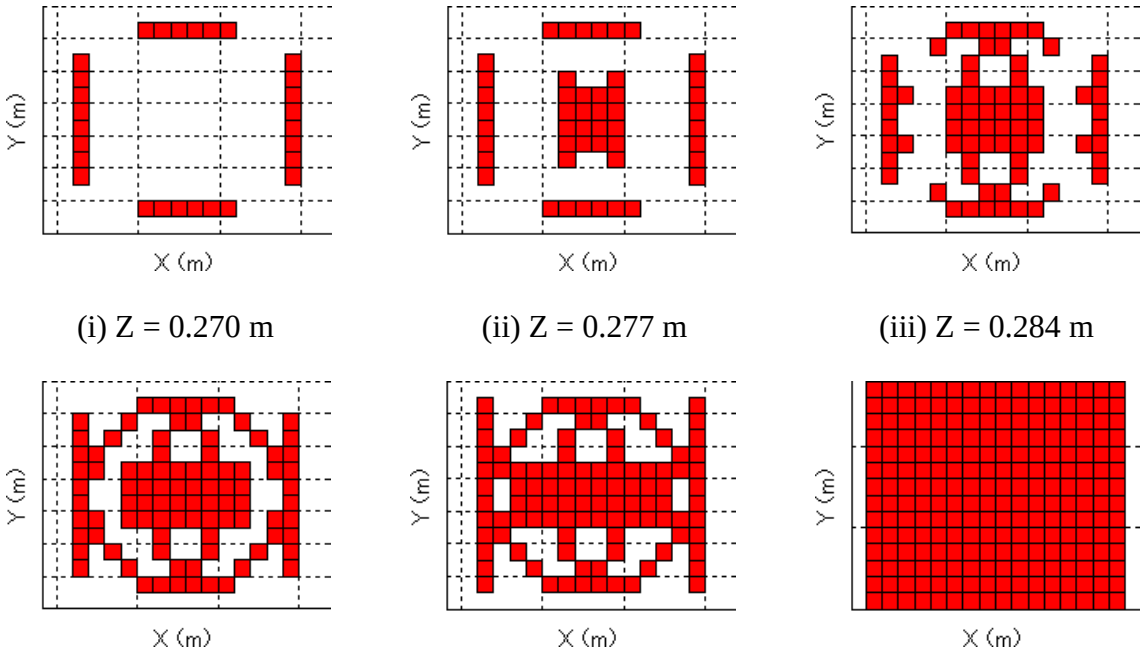

(i) Z = 0.270 m (ii) Z = 0.277 m (iii) Z = 0.284 m

(iv) Z = 0.291 m (v) Z = 0.298 m (vi) Z = 0.3 m (Plate)

(b) Cross-section in the plate-frame region

Fig. 9 Optimum TPS model including heat transfer effects

NOMENCLATURE

$\{f\}$ = global nodal force vector

$\{F_r\}$ = external force vector for the r^{th} natural mode

$[K]$ = global stiffness matrix

$[M]$ = global mass matrix

n = number of degrees-of-freedom

N = total number of degrees-of-freedom

P = correlation factor

$R_{j,\,l}$ = ratio between $\sigma_{j,\,l}^{vm}$ and $\sigma_{j,\,\max}^{vm}$

S_l^{multi} = multi-objective control parameter for the l^{th} element

W_j = j^{th} criterion weighting factor

$\{x\}$ = global nodal displacement vector

$\{\ddot{x}\}$ = global nodal acceleration vector

$\sigma_{j,\,l}^{vm}$ = j^{th} von Mises stress for the l^{th} element

$\sigma_{j,\,\max}^{vm}$ = maximum value of the j^{th} von Mises stress

α = parameter for the element removal

ω = natural frequency

$\{\Phi\}$ = natural mode

$\{\varepsilon\}$ = modal displacement vector

$\|\cdot\|$ = L^2 norm